Analysis of the critical components of flash drought using the standardized evaporative stress ratio

Stuart G. Edris [a,*], Jeffrey B. Basara [a,b], Jordan I. Christian [a], Eric D. Hunt [c], Jason A. Otkin [d], Scott T. Salesky [a], Bradley G. Illston [a,e]

[a] School of Meteorology, University of Oklahoma, Norman, Oklahoma, United States
[b] School of Civil Engineering and Environmental Science, University of Oklahoma, Norman, Oklahoma, United States
[c] Atmospheric and Environmental Research, Inc., Lexington, Massachusetts, United States
[d] Cooperative Institute for Meteorological Satellite Studies, Space Science and Engineering Center, University of Wisconsin-Madison, Madison, Wisconsin, United States
[e] Oklahoma Climatological Survey, University of Oklahoma, Norman, Oklahoma, United States

ARTICLE INFO

ABSTRACT

Flash droughts develop rapidly (~1 month timescale) and produce significant ecological, agricultural, and socioeconomical impacts. Recent advances in our understanding of flash droughts have resulted in methods to identify and quantify flash drought events. However, few studies have been done to isolate the individual rapid intensification and drought components of flash drought, which could further determine their causes, evolution, and predictability. This study utilized the standardized evaporative stress ratio (SESR) to quantify individual components of flash drought from 1979 – 2019, using evapotranspiration (ET) and potential evapotranspiration (PET) data from the North American Regional Reanalysis (NARR) dataset. The temporal change in SESR was utilized to quantify the rapid intensification component of flash drought. The drought component was also determined using SESR and compared to the United States Drought Monitor. The results showed that SESR was able to represent the spatial coverage of drought well for regions east of the Rocky Mountains. Furthermore, the rapid intensification component agreed well with previous flash drought studies, with the overall climatology of rapid intensification events showing similar hotspots to the flash drought climatology east of the Rocky Mountains. The rapid intensification climatology suggested areas west of the Rocky Mountains experience rapid drying more often than east of the Rocky Mountains.

1. Introduction

Drought is a climate extreme resulting from below normal precipitation and above normal temperatures over a prolonged period of time, which causes an imbalance in the hydrologic system (American Meteorological Society 1997; Pachauri et al., 2014). This puts stress on ecological systems and can have large socioeconomic impacts; extreme droughts can yield billions of dollars (US) of losses (Heim 2002; Dai 2011; NCEI 2017). Many studies have focused on being able to detect, monitor, and predict drought events. Historically, this has been accomplished through long term indices (~2 - 6+ month averages) such as the Palmer Drought Severity Index (PDSI; Palmer 1965) and Standardized Precipitation Index (SPI; McKee et al., 1993, McKee et al., 1995).

More recent studies have focused on drought events that undergo rapid evolution (~1 month), denoted as "flash drought" in Svoboda et al. (2002). Flash droughts differ from traditional droughts in several ways. While traditional drought can occur in any given season, flash drought has a distinct seasonality, favoring the growing season (Chen et al., 2019; Christian et al., 2019a; Noguera et al., 2020; Christian et al., 2021). Additionally, traditional drought can occur in any given region, while flash droughts tend to favor transition zones with a strong precipitation gradient (Kim and Rhee 2016; Chen et al., 2019; Christian et al., 2019b). Further, because of the rapid drying and desiccation of the land surface, flash droughts can have large ecological, agricultural, and socioeconomic impacts (Christian et al., 2020, Christian et al., 2022). Examples include the 2015 flash drought in the southern Great Plains (Otkin et al., 2019), the 2012 flash drought across the central United States (Otkin et al., 2016, 2018; Basara et al., 2019), the 2010 western Russia flash drought (Christian et al., 2020; Hunt et al., 2021), and the

---

1936 flash drought (Hunt et al., 2020; Bolles et al., 2021).

Because flash droughts develop over relatively short time periods, traditional drought monitoring, evaluation, and detection methods are generally unable to accurately capture rapid intensification events. Consequentially, there has been significant work focused on variables that respond quickly to a rapidly drying environment and have a high temporal resolution (e.g., ~1 week timescale) that allows them to detect the rapid onset of drought on shorter time scales (Lisonbee et al., 2021). While changes in the United States Drought Monitor (USDM) database (Chen et al., 2019) and the standardized evaporative precipitation index (SPEI) at a monthly timescale (Noguera et al., 2020) have been examined to determine flash drought, the main variables analyzed include soil moisture (e.g., Hunt et al., 2009; Ford et al., 2015; Otkin et al., 2019; Liu et al., 2020a; Osman et al., 2021) as well as evapotranspiration (ET) and potential evapotranspiration (PET; e.g., Otkin et al., 2013, 2014; Li et al., 2020; Kim et al., 2019; Hobbins et al., 2016; McEvoy et al., 2016; Kim et al., 2019; Vicente-Serrano et al., 2018; Christian et al., 2019b; Nguyen et al., 2019, 2021; Pendergrass et al., 2020; Osman et al., 2021). In particular, ET has been found to be one of the most sensitive variables to flash drought (McEvoy et al., 2016; Chen et al., 2019) and rapid decreases in ET can serve as a precursor for flash drought development, typically occurring about 1 – 2 weeks in advance of drought onset (Otkin et al., 2013; Chen et al., 2019). In addition, ET has been associated with the atmospheric supply of moisture available to the environment while PET is associated with the terrestrial demand for moisture (Hobbins et al., 2016; Christian et al., 2019b). Thus, many studies have focused on ET and PET, creating a number of standardized indices to measure drought such as the evaporative demand drought index (EDDI; Hobbins et al., 2016; McEvoy et al., 2016; Pendergrass et al., 2020), the standardized evapotranspiration deficit index (SEDI; Kim and Rhee 2016; Kim et al., 2019), the evaporative stress index (ESI; Anderson et al., 2007, 2013), the rapid change index (RCI; Otkin et al., 2014), and the standardized evaporative stress ratio (SESR; Christian et al., 2019b). Furthermore, ET is able to not only describe flash drought events, but it can also be used to examine drought in general, and capture historic drought events, including the 1934, 1954, 1988, and 2011 droughts (Kim and Rhee 2016; Kim et al., 2019).

With the addition of numerous studies examining flash droughts events and the creation of various indices to identify and quantify flash drought events, Otkin et al. (2018) proposed a general framework that required any flash drought definition to include two critical components. First, a rapid intensification component on the order of a month should be included given its importance in flash drought development (Liu et al., 2020a,b, ; Noguera et al., 2020) and impacts due to rapid desiccation of the terrestrial surface. Additionally, flash drought cannot occur unless drought conditions are achieved (Lisonbee et al., 2021). Thus, a drought component should be clearly identifiable whereby environmental indices fall below the 20th percentile of their distribution. Some studies have examined the climatology of these components, such as Liu et al., 2020a, Noguera et al., 2020, and Otkin et al., 2021. However, little work has been done to examine these two components individually.

Dividing flash droughts into these two components can be critical in determining several features associated with flash droughts. For example, quantifying the occurrence of rapid intensification can help improve understanding of flash droughts drivers, aid in their real time identification, and denote areas to improve the predictability of flash droughts. Therefore, this study utilizes the SESR method of identifying flash drought (Christian et al., 2019b) to (1) analyze the rapid intensification and drought components *individually*, (2) evaluate the ability of SESR to detect drought in general, (3) quantify the occurrence of rapid intensification and identify locations that experience rapid intensification but not drought, and (4) determine which of the two components is most critical for flash drought occurrence in space and time.

2. Material and methods

2.1. Data

2.1.1. North American regional reanalysis

This study utilized data from the North American Regional Reanalysis (NARR) which was designed to accurately represent the climate and hydrology of North America (Mesinger et al., 2006). The spatial resolution of the NARR is 32 km × 32 km with a 3-hour temporal interval. For this study, surface evapotranspiration (ET) and potential evapotranspiration (PET) for the growing seasons of 1979 to 2019 were incorporated into the analysis. PET was calculated within the Noah land surface model using the Penman equation with surface temperature, soil flux, radiation, windspeed, and specific humidity (Ek et al., 2003; Mahrt and Ek 1984). ET calculations used numerous moisture and vegetation variables (such as vegetation density, stomatal conductance, precipitation, soil moisture, etc.) to determine three components (evaporation from the soil, transpiration, and evaporation from canopy intercept), which are calculated separately and then summed to obtain the total ET (Ek et al., 2003; Chen et al., 1996). The NARR has been successfully utilized in multiple, previous flash drought analyses including Christian et al., (2019a, b), Chen et al. (2019), and Basara et al. (2019). In addition, this study refers to numerous locations that have similar climate and flora conditions by their geographic names. A guide to these geographic regions can be found in Supplementary Figure 1.

2.1.2. United States drought monitor

The USDM is a collaboration between numerous federal and state organizations and universities designed to monitor, identify, and convey information about drought to the public and stakeholders. It incorporates the professional opinions of the expert scientists who serve as drought monitor authors and who use numerous metrics (e.g., temperature, precipitation, streamflow, soil moisture, snowpack, ground water, and vegetation conditions; Svoboda et al., 2002). Because the USDM has been widely utilized for drought identification (e.g., Otkin et al., 2013, 2014; Ford et al., 2015; Chen et al., 2019), USDM drought values were incorporated into this study for evaluation of drought depicted by SESR. Because the data from the USDM are in a polygon format, it was rasterized in this study by comparing each NARR grid point to the polygon, and assigning the grid point the value of the polygon, similar to the method used in Chen et al. (2019). Further, this study was not concerned with abnormally dry events and as such, D0 drought was given the same value as non-drought conditions. In addition, the USDM provides a basis for categorizing drought intensity based on percentiles (i.e., Table 2 in Svoboda et al. (2002)). Because the USDM has evolved and refined its determination of drought over time, data was used from 2010 – 2019 to evaluate the SESR drought component. Finally, when compared to the USDM, the SESR drought component was averaged to the same weekly time scale as the USDM.

2.2. Standardized evaporative stress ratio

This study employs the flash drought identification method developed by Christian et al. (2019b), which incorporates surface moisture flux via ET (evaporation from the soil and transpiration from vegetation) and the atmospheric demand for moisture (PET). The ratio of ET to PET yields the evaporative stress ratio (ESR) defined in Christian et al. (2019b) as:

$$ESR = \frac{ET}{PET} \tag{1}$$

whereby ESR values range from 0 (a completely dry near-surface atmosphere) to 1 (a saturated near-surface atmosphere). Due to the diurnal variability of ESR, it is recommended to use ESR on daily or pentad time scales (Christian et al., 2019b); this study utilized

non-overlapping pentad (5-day) averages.

To better investigate flash drought events across different climate zones, the standardized evaporative stress ratio (SESR) was used.

$$SESR_{ijp} = \frac{ESR_{ijp} - \overline{ESR_{ijp}}}{\sigma_{ESR_{ijp}}} \tag{2}$$

The subscripts *i* and *j* refer to the *i*th and *j*th spatial grid point and the subscript *p* refers to the *p*th pentad in the Gregorian calendar (leap days excluded). Overbars indicate mean values, and σ refers to standard deviations. For this study, the mean and standard deviation values were calculated from the 41 years in the dataset. This standardization process allows the variable to be more easily compared across different regions as well as allows a more robust comparison of values over multiple years and across parts of the growing season for each grid point (Christian et al., 2019b). Negative values of SESR indicate a region is drier than normal, and a region is more moist than normal when SESR is positive. Changes in SESR were also computed to determine how SESR changes in time (whether the region is drying or moistening over time). The change in SESR is given by

$$\Delta SESR_{ij,p} = SESR_{ij,p+1} - SESR_{ij,p} \tag{3}$$

where the subscript *p* indicates the *p*th pentad. Note that ΔSESR should be calculated on the pentad timescale to better capture the trend in how SESR is changing. It is important to note that for this study, the change in SESR begins on the *p*th pentad. Thus, if a grid point has drying or moistening, it begins on the *p*th pentad and ends on the (*p*+1)th pentad. It should be noted that while ΔSESR was standardized in the original paper (Christian et al., 2019b), it was found that this second standardization did not impact the results and was thus omitted from discussion here.

Finally, evaporative demand is dramatically reduced in cold environments such that rapid drought development driven by evaporative stress is limited. As such, this study is restricted to the agricultural growing season (April – October) to focus on the favored season for flash droughts and similar to previous studies (Hunt et al., 2014; Otkin et al., 2014; Chen et al., 2019; Christian et al., 2019b; Noguera et al., 2020; Christian et al., 2021), with the domain set as the contiguous United States (CONUS).

2.3. Flash drought criteria

The method developed by Christian et al. (2019b) to identify flash drought using SESR is based on four specific criteria, which are used to identify rapid drying and drought conditions separately. They are:

1) The flash drought must be at least 30 days in length.
2) At the end of the flash drought, SESR must be at or below the 20th percentile for that grid point and pentad.
3) a) During the flash drought, ΔSESR must be at or below the 40th percentile for that grid point and pentad. b) No more than one exception is allowed for criterion 3a during the flash drought.
4) The temporal mean in ΔSESR during the whole rapid intensification period must be at or below the 25th percentile for that grid point and range of pentads.

For this study, each criterion was determined for each pentad in the dataset. To accomplish this, each day was treated as an "end date" for the flash drought. For the criteria analysis, a binary value of 1 (true, the criterion was satisfied for that pentad and grid point) or 0 (the criterion was not satisfied for that pentad and grid point) was given to each grid point and for each pentad, illustrated in Fig. 1 and is described in more detail in the following sections. Each criterion was determined for every pentad in the NARR dataset in order to examine SESR's representation of rapid intensification and drought independently.

An example of how these criteria identify flash drought is illustrated in Fig. 2. In this example, from Christian et al., 2019b, rapid intensification began on June 11, where ΔSESR was at the 26th percentile. The following two pentads were also below the 40th percentile, fulfilling criterion 3a. On the fourth pentad within the intensification period (labeled P4), the percentile increased above the 40th percentile, but subsequently continued below the 40th percentile. Because the increase in ΔSESR only lasted for 1 pentad, it fulfilled the condition for being a moderation period and not a termination of the rapid intensification period (criterion 3b). Finally, after the sixth pentad (labeled as P6), ΔSESR increased to be at the 58th percentile and remained above the 40th percentile on the following (eighth) pentad, signaling the end of the intensification period at July 11, after the sixth pentad. Finally, as the intensification period encompassed 6 pentads (30 days), criterion 1 was
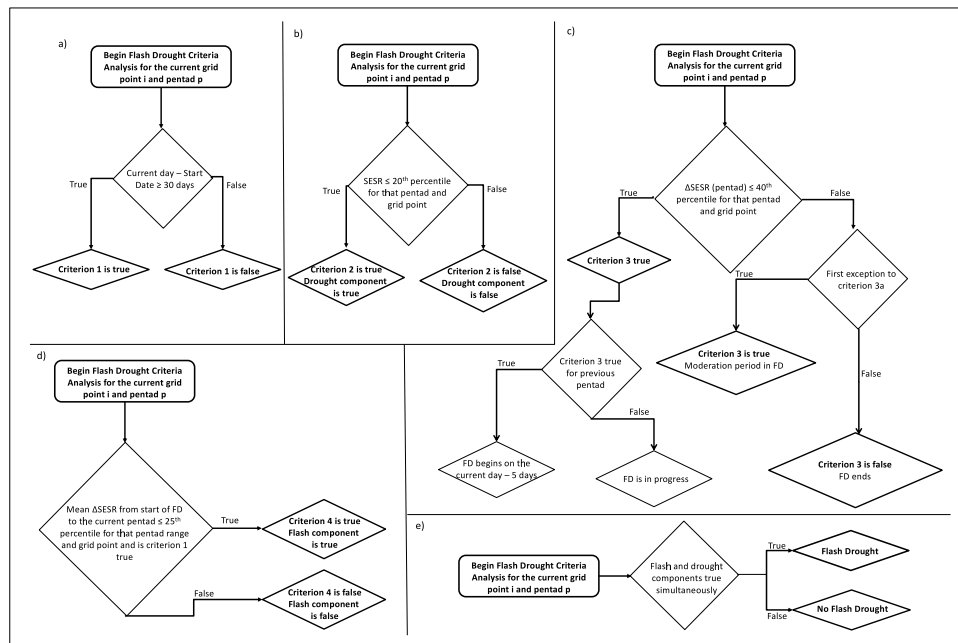

Fig. 1. Flow chart of flash drought detection. Flow chart showing the algorithm used for this study and how it calculated a) Criterion 1, b) Criterion 2 and the drought component, c) Criterion 3, d) Criterion 4 and the rapid intensification component, and e) flash drought. FD in the flow chart stands for flash drought.
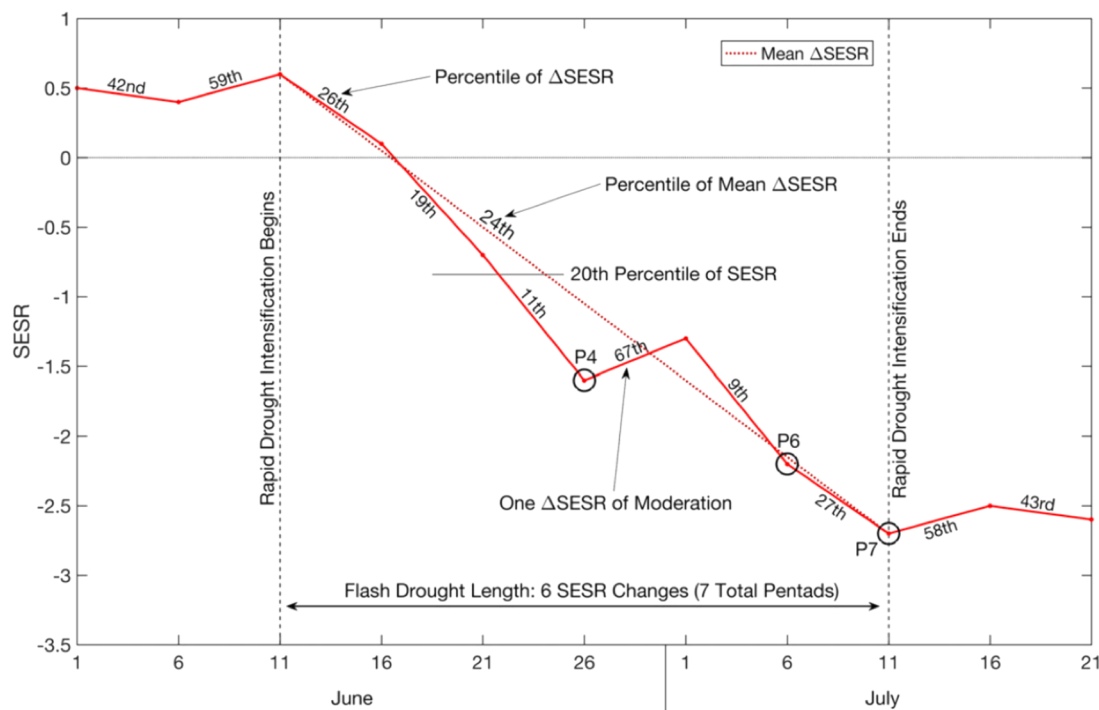
Fig. 2. Flash drought detection example. A time series schematic illustrating the four criteria used in the flash drought identification method. The fourth, sixth, and seventh pentads after the start of the rapid intensification period are labeled (P4, P6, and P7 respectively). [Fig. and caption from Fig. 2 in Christian et al., 2019.]

satisfied. In addition, the mean ΔSESR over the 6 pentads that characterized intensification period was at the 24th percentile, when compared to that same mean over all other years, satisfying criterion 4. Lastly, at the end of the intensification period, SESR was below the 20th percentile (which was around -0.8 in this example), indicating the region was in drought and fulfilling all the conditions of flash drought (Christian et al., 2019b).

2.4. Rapid Intensification component

For this study, the rapid intensification component is defined by the truth value of criterion 4, whereby rapid intensification occurs when criterion 4 is true. By extension, a rapid intensification event is said to have happened when criterion 4 is true. Criterion 1 is used to prevent the overall flash drought algorithm from identifying short-term "dry spells" as flash droughts. The algorithm checks whether the difference between the current day (plus five days, because criterion 3 considers ΔSESR which ends on the $(p+1)^{th}$ pentad) in the algorithm and the start of the flash drought is greater than 30 days (6 pentads). This means that criterion 1 is only true whenever rapid drying has almost continuously occurred, with a moderation period allowed, for at least 30 days. Note this also means that the algorithm identifies the near continuous rapid drying at the end of a specific drying period. For example, in Fig. 2, where the flash drought identified was 30 days in length (from June 11 to July 11), the algorithm would only identify criterion 1 as true on July 11 and later if the rapid intensification continued.

Physically, criterion 3 checks for rapid drying over a grid point. For a standardized change variable, the 50th percentile is approximately 0 and it represents no change in conditions for a given location and pentad. As such, requiring that ΔSESR be at or below the 40th percentile means this criterion is checking whether SESR is decreasing between two pentads. Even so, criterion 3 allows an exception in the event moderation of evaporative stress occurs during the flash drought development. For example, if a light precipitation event occurs over a grid point experiencing flash drought, the precipitation could slow how quickly SESR decreases (or even make it increase), but not enough to prevent the flash

drought from occurring over longer time periods. Further, because this criterion identifies rapid drying from pentad to pentad, it can be used to determine when the flash drought begins and ends. This can be seen in the example shown in Fig. 2.

Finally, criterion 4 is the last criteria designed to examine whether rapid drying is occurring over a grid point. Specifically, this criterion checks the overall drying between the start and end of the rapid drying period and determines if it was large enough to be considered a rapid intensification of drought conditions. An example is shown in Fig. 2, where the mean in ΔSESR (dashed red line) is below the 25th percentile. Note that this criterion infers the magnitude of the drying at the end of the rapid intensification by checking the magnitude of decreasing SESR. Additionally, the algorithm requires criterion 1 to be true for criterion 4 to be true, to ensure that only means over 6 pentads or more (the full rapid intensification period) are considered. This also dictates that criterion 4 depends on criteria 1 and 3 (both of which measure rapid drying components). Further, because criterion 4 also has its own determination for rapid intensification, it then represents all the parts of rapid intensification.

2.5. The drought component

The drought component (DC) was defined via criteria 2 which is the simplest criterion to determine and interpret. For flash drought to occur, the variable being used to identify it must be below the 20th percentile for that region and pentad to be considered in drought (Svoboda et al., 2002; Otkin et al., 2018). In addition, a critical aspect of this study was to more explicitly determine how well SESR represents drought in general, both in spatial coverage and intensity. The drought coverage represents where drought is present (and can thus be defined as the drought component), whereas the drought intensity provides additional information on the scale, strength, or impact of the drought. The drought intensity was identified and classified using SESR percentiles and the classification method provided by the USDM (Table 1). Because this study focuses on examining the components of flash drought, the drought component was determined and analyzed for every pentad in

Table 1

Percentiles used to determine drought categories (i.e., the drought intensity) with SESR. Percentiles are based on those used in the U.S. Drought Monitor (Svoboda et al., 2002).

Drought Category	Percentile Range
No Drought	21 – 100
Category 1	11 – 20
Category 2	6 – 10
Category 3	3 – 5
Category 4	< 2

the NARR dataset.

2.6. Statistical analysis

Statistical analyses of the rapid intensification and flash droughts were desired to determine where regions of rapid intensification occur, but may not fall into drought and how often this occurs. To this end, a contingency table and threat scores were used. For the contingency table or truth table, only two scenarios are considered. One is the frequency of rapid intensification events without flash drought and the other is the frequency of rapid intensification with flash drought, both relative to the total number of rapid intensification events. The other two scenarios have trivial results as the flash drought is not identified when there is no rapid intensification by definition. Equitable threat score time series were also used to show the occurrence of rapid intensification events that fall into drought relative to the total number of rapid intensification events. The equitable threat traditionally measures the skill of a model by comparing the number of correct forecasts from a truth table to the misses and false alarms. In this case, there are no false alarms (there cannot be flash drought events without rapid intensification), the misses are the rapid intensification events that do not reach drought, and "correct forecasts" are the rapid intensification events that become flash droughts. To this end, the equitable threat score then becomes a measure of rapid intensification events that become flash droughts relative to the total number of rapid intensification events. To test the robustness of the results, composite mean difference and Pearson correlation coefficient analyses were also performed and found similar results (not shown).

A contingency table was also used to compare the SESR drought component and USDM to examine how often SESR may identify a false positive or a false negative relative to the USDM. In addition, composite mean differences and Pearson correlation coefficient were also calculated to compare the SESR drought component with the USDM. A composite mean difference is the difference between to variables that have been average (in this case the average in time). The comparison then describes which of the two variables is greater and by how much. For this study, the difference was taken as drought identified by SESR minus USDM drought. For these analyses, the percentiles of SESR were averaged to the same weekly timescale as the USDM data, and the drought intensity was obtained from Table 1. Because the composite difference is the SESR drought component minus the USDM, positive values indicate that SESR predicted either more intense drought than the USDM, more frequent drought than the USDM, or it predicted false positives (SESR identified drought where there the USDM did not). Conversely, if the composite mean is negative, then SESR either underpredicted the strength of the drought, the frequency of the drought, or SESR failed to predict drought where it should have (misses). In order to determine which of these possibilities is true, these statistical comparisons were made for both drought intensity and coverage. For example, higher magnitudes in the composite difference for drought intensity comparisons while having smaller magnitude for the drought coverage would suggest that SESR is identifying where the drought is but is underestimating or overestimating the intensity of the drought depending on the sign of the composite difference. In this study statistical significance was determined using the Monte-Carlo bootstrapping method, which repeats a statistical calculation N times with the dataset shuffled to obtain a distribution. The original statistic is compared to that distribution in order to determine the significance. For this study, N = 5000 iterations was used.

3. Results

3.1. Case studies

To examine the performance of the algorithm with respect to rapid intensification and to compare the drought component with the USDM for specific flash drought events, several known cases were analyzed. U. S. flash droughts from 2011 and 2012 were chosen because they are well-studied events (e.g., for 2011 see Otkin et al., 2013, Ford et al., 2015, McEvoy et al., 2016, Vicente-Serrano et al., 2018, and Osman et al., 2021; for 2012 see Otkin et al., 2016, McEvoy et al., 2016, Basara et al., 2019, and Osman et al., 2021).

3.1.1. 2011: southern United States

During 2011, widespread and severe drought rapidly spread across much of the southern U.S. during the growing season, with the largest impacts focused on Texas and Oklahoma (Otkin et al., 2013; Ford et al., 2015; McEvoy et al., 2016; Vicente-Serrano et al., 2018). With respect to rapid intensification during 2011, SESR identified areas of flash drought in parts of Texas and Oklahoma during May of 2011 that spread in that region during June and propagated to the northeast as time progressed into August and September (Fig. 3). The identification of rapid intensification in central Oklahoma and north central Texas agrees with other studies using other datasets (Otkin et al., 2013; Ford et al., 2015; McEvoy et al., 2016). The timing of flash drought identified in May with additional intensification events in June also agreed with results of previous studies (McEvoy et al., 2016). Thus, SESR successfully identified rapidly drying conditions in central Oklahoma and north central Texas during April into May. Little intensification occurred during May and early June in eastern Oklahoma and Arkansas due to some moderating precipitation events, but the dry conditions expanded in June and July and propagated north and east in the following months into the Corn Belt area, agreeing with the results of Flanagan et al. (2017). In addition, Fig. 3 shows SESR was able to identify the spatial extent of the drought but also underestimates the intensity of the drought, particularly in Texas.

Figs. 4 and 5 show the correlation and composite mean difference between the drought component and USDM. Overall, SESR was well correlated with the drought identified by the USDM, with the correlation being statistically significant in most places except Texas, where it continuously underestimate the intensity of the drought and the correlation of the drought coverage was undefined due to persistent drought throughout the growing season. Additionally, some disagreement existed across Georgia, Texas, and locations further west into New Mexico and Arizona, whereby the intensity of the drought was underestimated (Fig. 5). That is, the composite difference for drought intensity is more negative than if just coverage is considered, implying SESR underestimated the intensity of the drought. The composite difference for spatial coverage of drought in Fig. 5 is negative for the Southern Plains and Georgia. Thus, SESR identified drought less frequently than the USDM. That is, there were weeks where SESR may not have identified drought whereas the USDM did identify drought for most weeks, thereby yielding the net negative difference in the spatial coverage comparison. This is possibly due to moderating influences (such as precipitation). Fig. 4 does show one potential weakness in the correlation coefficient. In regions where the drought coverage is continuous throughout the growing season, the variation in drought coverage is 0, which makes the Pearson correlation coefficient undefined. This can be seen in Texas in 2011 (Fig. 4). However, based on Fig. 3 and the small composite difference in Fig. 5, SESR was able to capture the spatial coverage of drought, agreeing with previous studies on ET's ability to represent
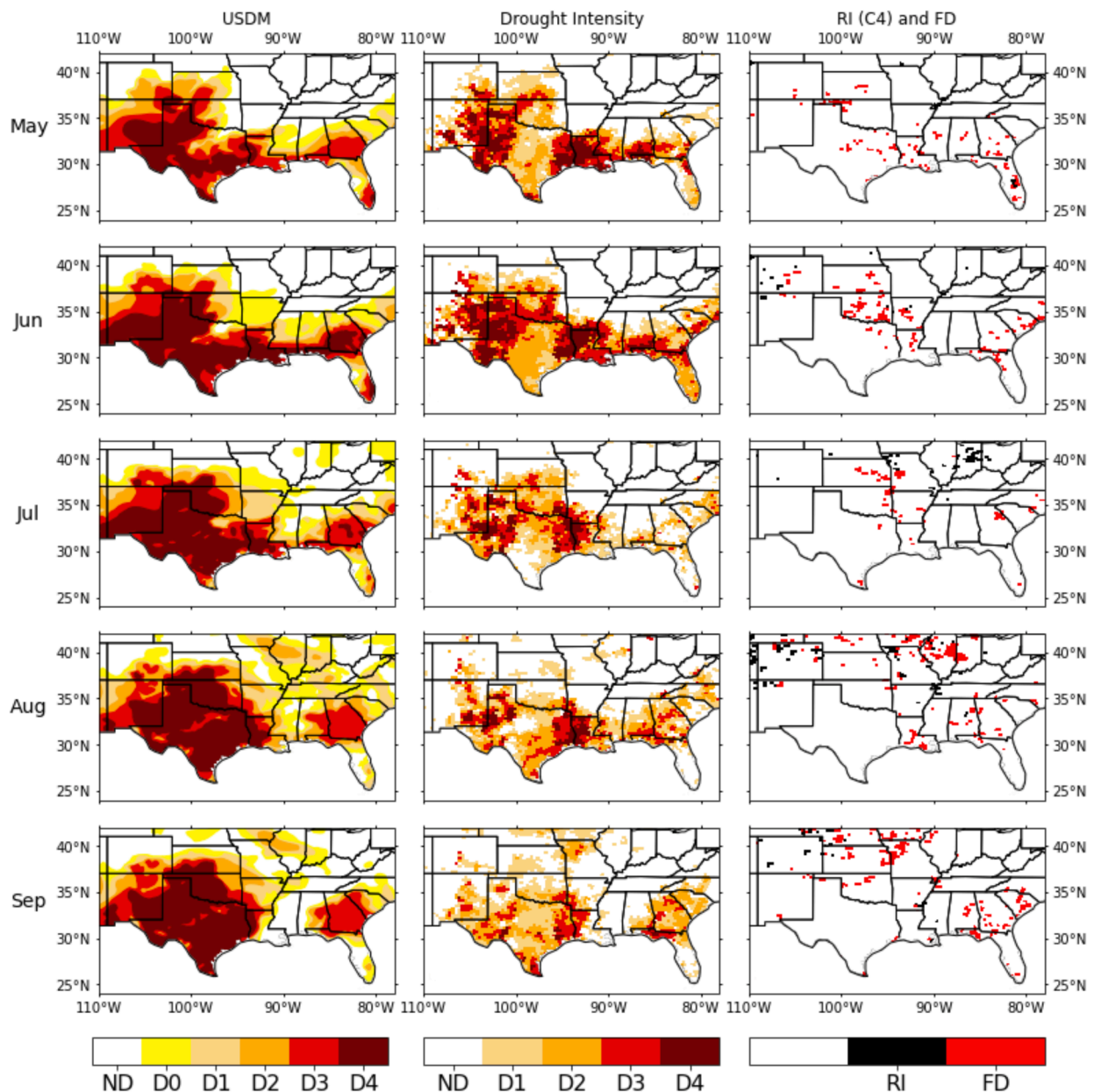
Fig. 3. Case study for the growing season of 2011 (excluding March, April, and October). (left) Drought identified by the USDM for the last week of the month, (center) monthly-averaged SESR drought intensity, and (right) monthly coverage of rapid intensification (RI) and flash drought (FD). Black/red color indicates SESR rapid intensification component/flash drought was newly identified for at least 1 pentad in that month. CX refers to the criterion used to identify the flash drought component. Some months (April and October) have been omitted for better readability.

drought (e.g., Otkin et al., 2013, McEvoy et al., 2016, and Vicente-Serrano et al., 2018).

Overall, SESR depicted drought spreading through most of west Texas and Louisiana in May, with expansion across most of the Deep South during June and July. Additionally, SESR identified exceptional drought for west Texas and Louisiana, but not to the extent identified by the USDM. This would explain the low correlation, as the USDM had exceptional drought (D4) for most of Texas and the Deep South, and D3 in Georgia. Thus, SESR did not identify some of the more extreme areas of drought during 2011 relative to the USDM. This is reflected in Sup. Fig. 2, which shows SESR and the USDM recorded similar scale drought coverage ($2 \times 10^6 - 2.8 \times 10^6$ km^2 or about 37% - 52% of the subregion in Fig. 3), however SESR found extreme (D3 and D4) drought much less frequently. However, the spatial coverage of the drought that SESR identified is very similar to the drought coverage in other studies (Otkin

et al., 2013; Kim and Rhee 2016; McEvoy et al., 2016; Vicente-Serrano et al., 2018). Thus, SESR was able to identify the spatial coverage of the drought. It also identified regions where the drought was most intense (though not necessarily the scale of the intensity).

3.1.2. 2012: central and midwestern United States

During 2012, a large and severe drought event spread across the Central U.S. with large impacts on the Corn Belt and upper Mississippi River (Otkin et al., 2016; Ford et al., 2015; McEvoy et al., 2016; Basara et al., 2019). Rapid drought intensification began in May across central Kansas and northern Missouri and steadily spread into Nebraska in June, and to the rest of the Corn Belt in July (Fig. 6). These results are in agreement with Basara et al. (2019), McEvoy et al. (2016), and Otkin et al. (2016). More specifically, the algorithm yielded the individual regions that experienced rapid intensification found in Basara et al.
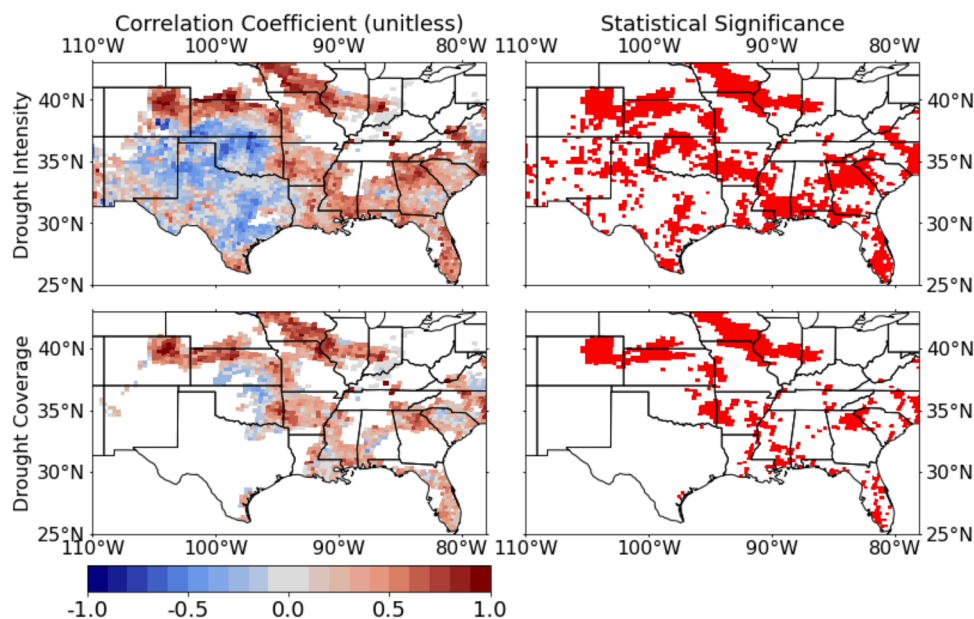
Fig. 4. Correlation coefficient of the SESR drought component with the USDM using weekly data for April – October of 2011. (left) Correlation coefficient between the SESR drought component and USDM, and (right) the 95% statistical significance, calculated using the Monte-Carlo method with N = 5000. Statistical comparisons are for (top) drought coverage and intensity and (bottom) only drought coverage.
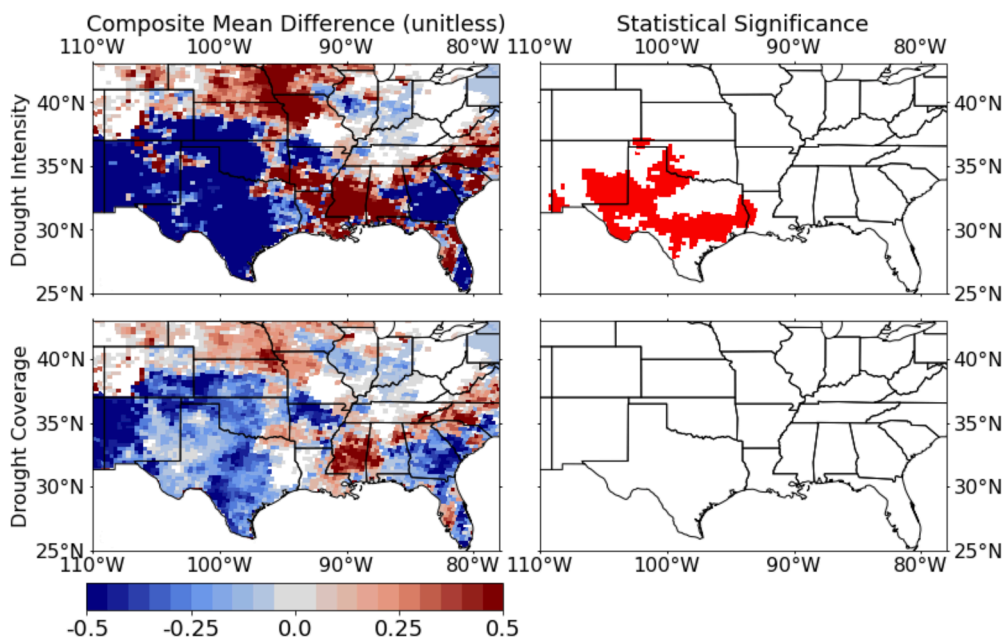

Fig. 5. Composite mean difference between the SESR drought component and the USDM using weekly data for April – October of 2011. (left) Composite mean difference between the SESR drought component and the USDM, and (right) the 95% statistical significance, calculated using the Monte-Carlo method with N = 5000. Statistical comparisons are for (top) drought coverage and intensity and (bottom) only drought coverage.

(2019), such as north central Kansas in May, north central Oklahoma in June, north central Missouri in May, central Nebraska in June, and southeast Minnesota in August. Additionally, the algorithm identified rapid intensification in some regions not previously discussed in connection with the 2012 drought such as southern Texas, and isolated parts of the Deep South. SESR also showed that it was able to represent the spatial coverage of the drought, but there was again a discrepancy in its representation of the intensity of the drought.

Similar to the 2011 case, SESR was correlated to the drought identified by the USDM, with that correlation generally being statistically significant. But it underestimated where the drought in Georgia and the

Central Plains, where it was most intense (Fig. 7). In particular, it tended to underestimate persistence of the drought slightly in the Central Plains or failed to identify drought altogether, primarily in Georgia (Sup. Fig. 3). This is more prominent west of the Rocky Mountains (with some of the reason discussed in Sec. 4). But the monthly average (Fig. 6) tends to agree relatively well with the drought coverage for 2012, agreeing with Otkin et al., 2014 and McEvoy et al., 2016. Therefore, SESR had more trouble capturing the persistence of the drought from week to week rather than the spatial coverage east of the Rocky Mountains. This week to week variation in SESR is likely the cause of the low correlation in drought correlation in Fig. 7 and the negative difference in Sup. Fig. 3.
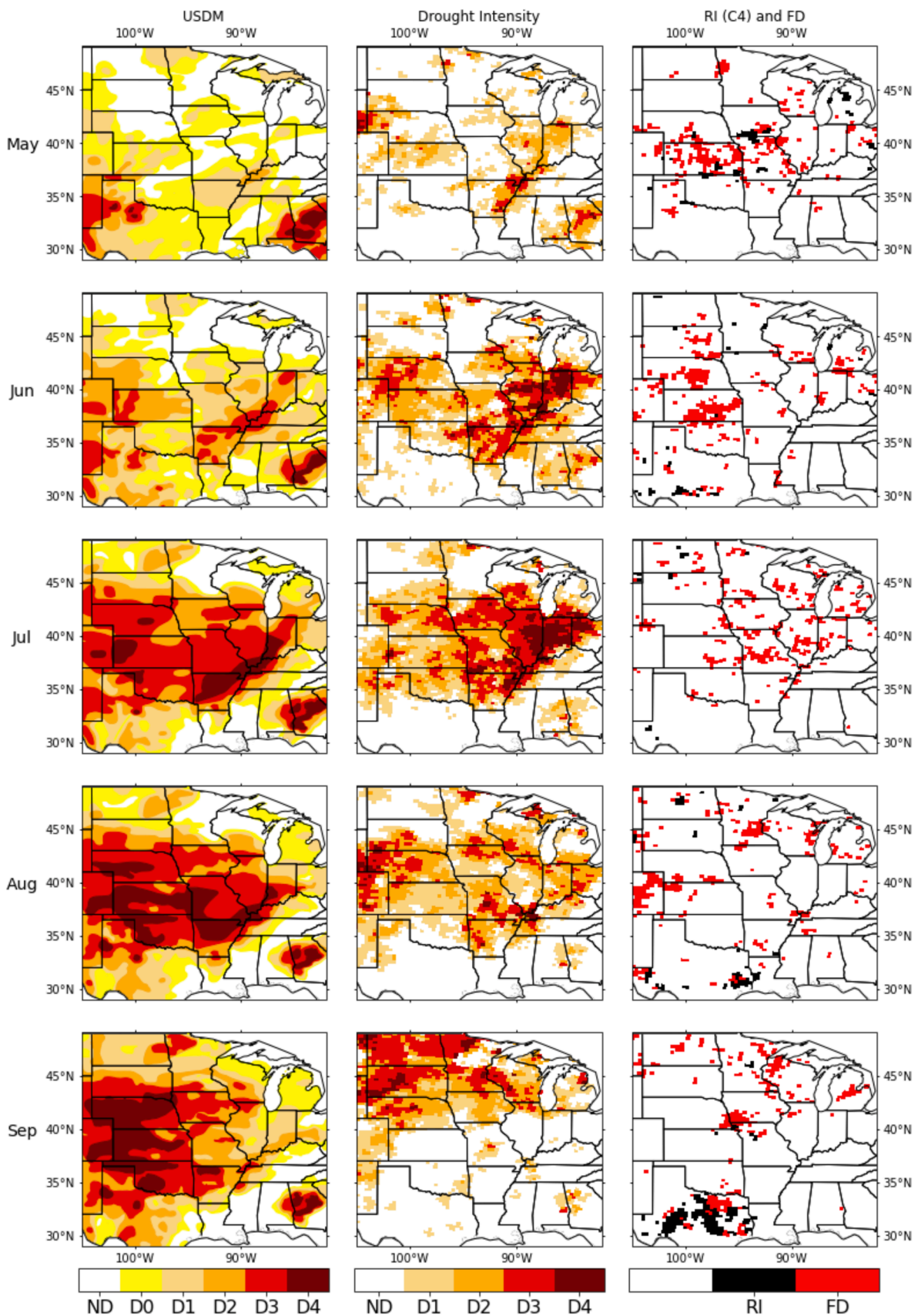
Fig. 6. Case study for the growing season of 2012 (excluding March, April, and October). (left) Drought identified by the USDM for the last week of the month, (center) monthly-averaged SESR drought intensity, and (right) monthly coverage of rapid intensification (RI) and flash drought (FD). Black/red color indicates SESR rapid intensification component/flash drought was newly identified for at least 1 pentad in that month. CX refers to the criterion used to identify the flash drought component. Some months (April and October) have been omitted for better readability.
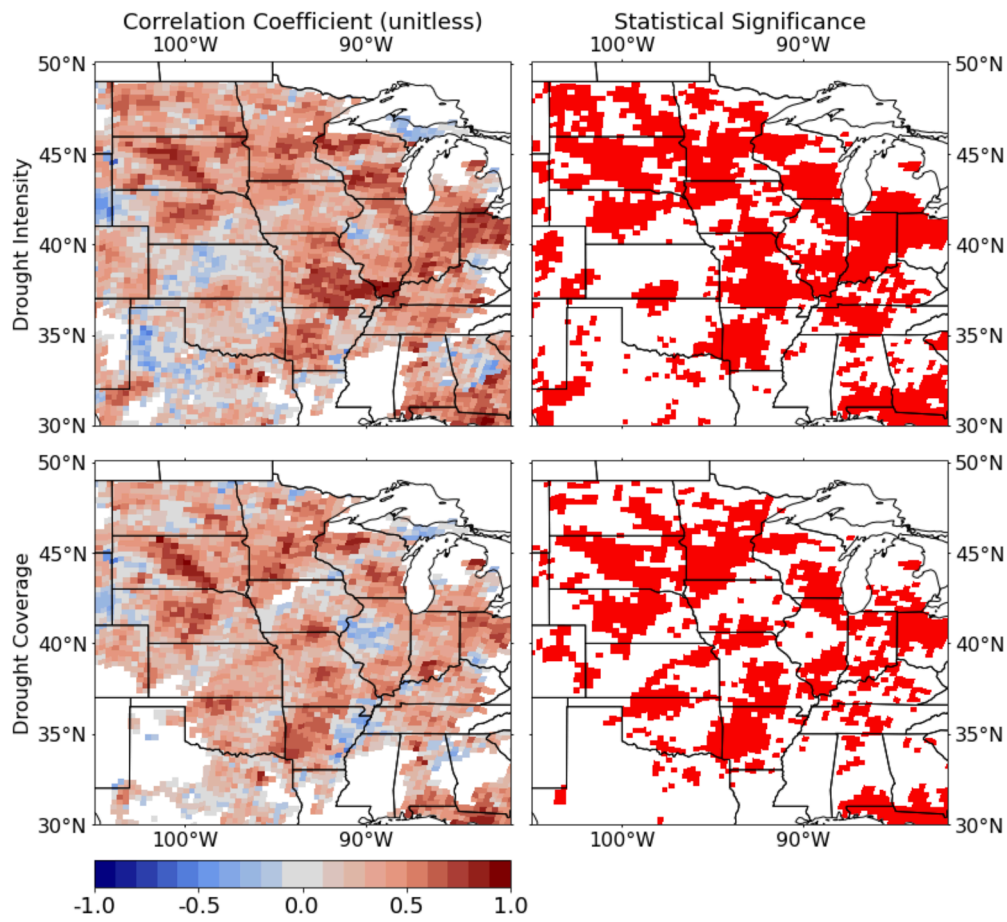
Fig. 7. Correlation coefficient of the SESR drought component with the USDM using weekly data for April – October of 2012. (left) Correlation coefficient between the SESR drought component and USDM, and (right) the 95% statistical significance, calculated using the Monte-Carlo method with N = 5000. Statistical comparisons are for (top) drought coverage and intensity and (bottom) only drought coverage.
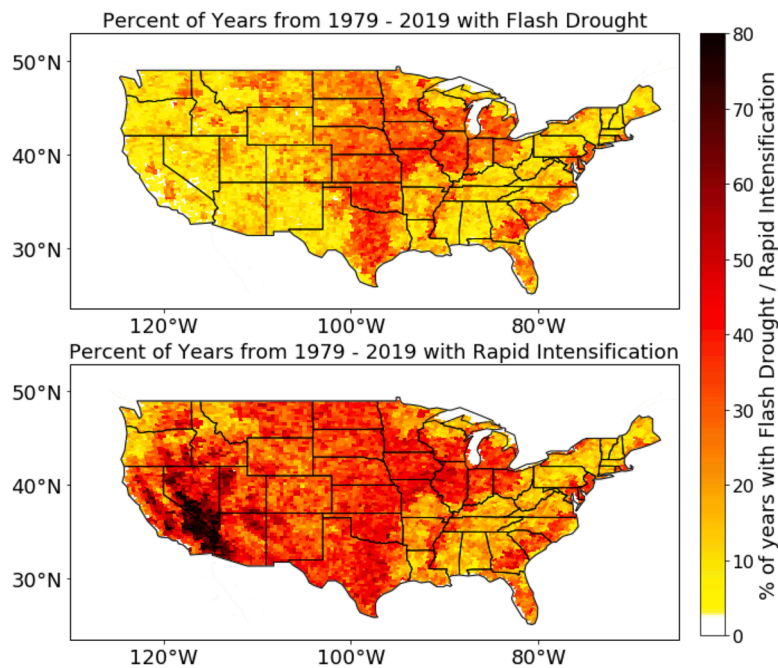

Fig. 8. Climatological average (from 1979 – 2019) of flash drought frequency (percentage of years with flash droughts; top) and the frequency of the rapid intensification component (bottom).

In addition, SESR underestimated the severity of the drought in most locations, particularly where the drought was most severe in the lower Ohio River Valley and Central Plains.

Examining Fig. 6, minimal drought coverage occurred during May (2 $\times 10^6$ km^2 or about 43% of the subregion in Fig.; Sup. Fig. 4), except for along the upper Mississippi delta, following the above normal precipitation at the start of the growing season (Basara et al., 2019). However, as time proceeded, the drought worsened and spread eastward into the upper Mississippi River region and lower Ohio River Valley in June, intensified in these regions, and spread into western Iowa and the Corn Belt region during July and August. The drought coverage maximized around 3.5 $\times 10^6$ km^2 (about 62% of the subregion) according to the USDM and 2.8 $\times 10^6$ km^2 (about 54% of the subregion) according to SESR. Again, SESR tended to identify D2 and occasionally D3 drought with some D4 drought in Indiana and surrounding states, whereas the USDM identified widespread D3 and D4 drought for this event. In addition, SESR indicated that the drought spread northwestward into the Dakotas much faster than was indicated by the USDM. Hence, while SESR may not identify the severity of the drought, it continued to capture the spatial extent and regions experiencing significant drought effectively (Fig. 6).

3.2. Climatology

3.2.1. SESR rapid intensification

The first part of the climatological analysis focused on rapid intensification. The rapid intensification and flash drought climatologies are displayed in Fig. 8. Given that the flash drought climatology was based on the method of Christian et al. (2019b), the analysis was consistent in identifying hotspots in the Great Plains, the Yazoo Delta, the Coastal Plains, and various areas along the East Coast. The hotspots are located around various precipitation gradients and/or agricultural regions, in agreement with previous studies (Chen et al., 2019; Christian et al., 2019b, Otkin et al., 2021). The rapid intensification analysis displays similar hotspots with an increased annual frequency of about 10% - 20%. However, an additional expansive hotspot in the rapid intensification was located across the Desert Southwest, and into central Nevada. Further, other areas in the Intermountain West, including Central Valley and Great Salt Lake and surrounding areas yielded a higher frequency of rapid intensification not highlighted in the flash drought climatology. Overall, regions of rapid intensification occurred more frequently than flash drought as expected given rapid intensification is only one component of flash drought development. However, east of the Rocky Mountains rapid intensification is more closely linked to flash drought

development while west of the Rocky Mountains and in the Desert Southwest there are frequent rapid intensification events (more frequently than east of the Rocky Mountains) but with few events reaching drought status and achieving flash drought development (see Sec. 4 for the reason).

To examine areas with rapid intensification but no drought, a contingency table analysis was performed to examine the frequency of rapid intensification events that both do and do not fall into drought (Fig. 9). The analysis confirms that most of the rapid intensification events east of the Rocky Mountains correspond with drought. However, west of the Rocky Mountains and the more arid regions of western Texas experience more rapid intensification events without going into drought. This result is also displayed in Fig. 10, where the difference in areal coverage for rapid intensification and flash drought decreases when only the area "east" of the Rocky Mountains is considered (i.e., east of 105W). A benefit of using the binary values is that the areal coverage of each component can be easily calculated by summing over all the grid points in a domain (at any time scale desired, such as pentad, weekly, monthly, or yearly), and multiplying by the areal coverage of each grid point (32 km × 32 km for the NARR grid), as seen in Fig. 10. Fig. 10 indicates that for locations east of the Rocky Mountains, the temporal peak in flash drought and rapid intensification events occurs in July and August which agrees with the seasonality of flash drought noted by Chen et al. (2019), Christian et al. (2019b), Noguera et al. (2020), and Otkin et al. (2021). Finally, the climatologically averaged threat score (Sup. Fig. 5) was also higher, by about 0.1 on average, for just the eastern U.S. when compared to CONUS. The eastern U.S. threat score also showed a maximum in the summer season, occurring with the seasonally favored time for flash droughts. In addition, correlation coefficient and composite mean difference analyses were performed on the rapid intensification and flash drought events and showed identical results (not shown). Thus, these results show that rapid intensification plays the prominent role in determining flash drought development east of the Rocky Mountains, whereas the drought component plays a more prominent role west of the Rocky Mountains.

3.2.2. SESR drought component

The second part of the climatological analysis focuses on the overall performance of the SESR drought component. The climatology of the drought component was found to be about 0.2 (20%) everywhere, by the definition of criterion 2. The results of the comparisons between the USDM and drought component for all years (2010 – 2019) is shown in Fig. 11. The comparisons were performed on the same weekly timescale as the USDM dataset. Across the Intermountain West, the composite
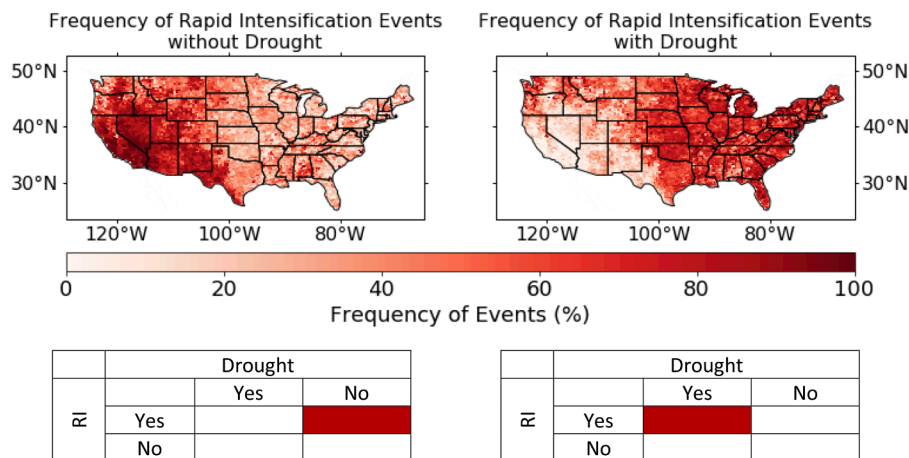

Fig. 9. Frequency of rapid intensification and flash drought events. Frequency of rapid intensification events that (left) do not fall into drought and (right) do fall into drought, relative to the total number of rapid intensification events. The frequencies were calculated for the growing season of the 1979 – 2019 period. The contingency table below shows the frequency to the corresponding map above it.
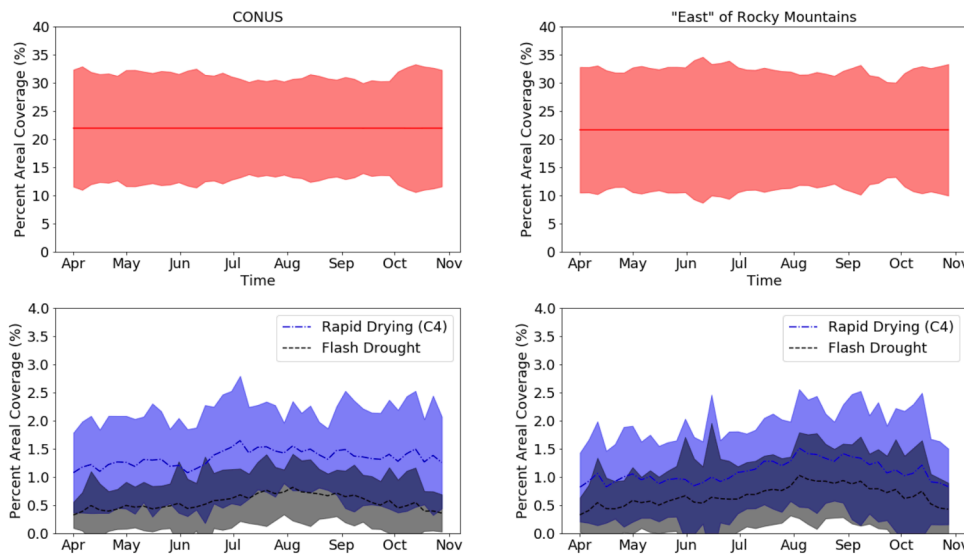
Fig. 10. Average time series of flash drought components. The annual average percentage of areal coverage for drought (top, red line), rapid intensification (bottom panel, blue line), and flash drought (bottom panel, black line) spanning 1979 – 2019 in time for the whole domain (U.S.; left) and across the domain east of 105W to exclude the Intermountain West (right). Shaded areas denote 1 standard deviation variability for drought coverage (red), rapid intensification (blue), and flash drought (grey). Dark blue shading is where the variability in rapid intensification and flash drought overlap.
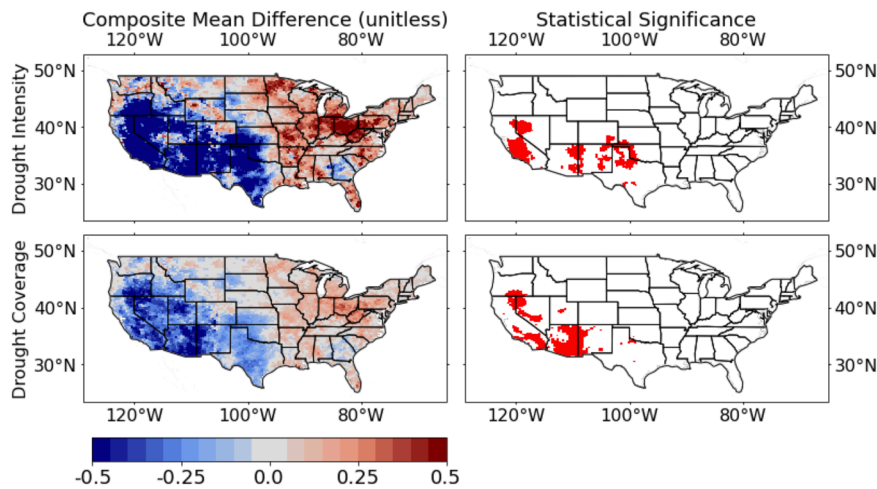

Fig. 11. Composite mean difference between SESR drought component and USDM for the 2010 – 2019 growing seasons. Composite mean difference (left) between the SESR drought component and USDM and statistical significance (right) for the corresponding composite difference for coverage and intensity (top) and just drought coverage (bottom) for April – October of 2010 – 2019.

mean difference between the USDM and drought component (Fig. 11) illustrates that SESR has difficulty identifying drought within the region, often failing to identify drought when one occurs (bottom panels). This could be due to the fact that the USDM is focused on a more long-term drought (i.e., different type of drought) as compared to SESR (see Section 4). Further, when it does identify drought in the Intermountain
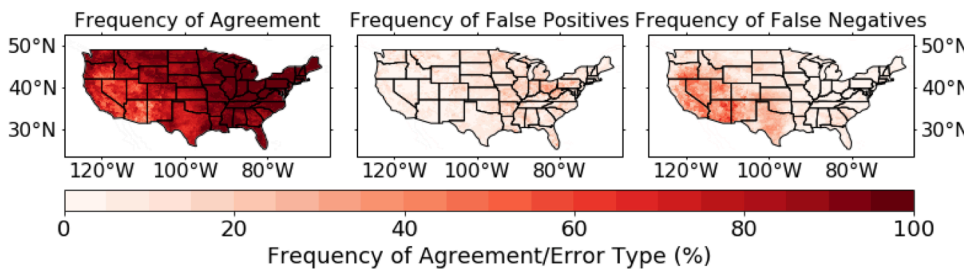

Fig. 12. SESR drought component and USDM contingency table analysis for the 2010 – 2019 growing seasons. Spatial distribution of averaged agreement of drought (SESR drought component and USDM both identified or did not identify drought at the same time; left), false positive error (center), and false negative error (right). The Fig. was determined by calculating the mean in the corresponding contingency table below the map for each grid point. The mean was performed across each week in April – October during 2010 – 2019 period.

West, it tends to underestimate the intensity of the drought (hence the stronger mean difference in the top panels). Conversely, in the Ohio River Valley SESR tends to overestimate the intensity of drought. In contrast to this, the composite difference is small and near zero (no difference, SESR identifies drought well) in the Northern and Central Great Plains, Pacific Northwest, as well as parts of the Deep South. An additional note is that there is no statistical significance in the composite mean difference except where the difference is fairly large in the Intermountain West. This further demonstrates SESR's ability to identify drought as there is no statistically significant difference between drought identified by the USDM and by SESR.

To quantify the spatial coherency of drought identification between SESR and the USDM a contingency table analysis was performed for each pentad and grid point. The results display the frequency of correct drought identification by SESR when compared to the USDM (Fig. 12; left panel). A critical result of the analysis is the notable agreement between the USDM and SESR that consistently occurred across the majority of the U.S., particularly east of the Mississippi River and Pacific Northwest. Further, weaker to neutral agreement occurred in the semi-arid Great Plains (namely the Southern Great Plains), portions of Georgia, and the Intermountain West with frequent disagreement in the arid Desert Southwest.

Fig. 12 provides the frequency of false positive and false negative errors respectively. When compared with the results of the composite mean difference (Fig. 11), SESR more frequently arrived at a false negative (or a "miss") whereby it failed to identify drought when needed in the semi-arid to arid regions and portions of Georgia. This could explain the negative composite difference found in the Southern Great Plains and around the more arid regions. However, more false positives (or "false alarms") were identified by SESR east of the Mississippi River centered around the Great Lakes region and the Ohio River Valley. An additional possibility is that SESR becomes a good indicator of drought in regions where there is moderate to high transpiration from the vegetation, so that the ET and PET become a more accurate measure of vegetative stress. This would also explain the high negative composite difference in the Intermountain West and Southern Plains, where the vegetation retains moisture in the arid environments, but works well in the Northern Plains and Pacific Northwest, where the agricultural crops and temperate vegetation transpire at a moderate rate. However, this does not explain the poor performance in Georgia and the Ohio River Valley, and additional research needs to be done to determine the reason for this.

4. Discussion

SESR was able to successfully capture the rapid intensification component shown in previous case studies (e.g., Otkin et al. (2013) and McEvoy et al. (2016) in 2011 and Basara et al. (2019) in 2012). Climatologically, the rapid intensification component occurs commonly in agriculturally-dominated land areas east of the Rocky Mountains, but also frequently occurs west of the Rocky Mountains, especially in the Desert Southwest (Fig. 8). While rapid intensification events that do not reach drought status do occur in the eastern half of the United States, they are uncommon (Fig. 9). However, west of the Rocky Mountains, rapid intensification events occur often but few flash droughts events are identified. This suggests that the critical factor in this region is the drought component. There may be several reasons for this dichotomy. For example, in the western United States the rapid intensification events may be due to the climatological onset or termination of the seasonal monsoon conditions in that region. As such, precipitation is often followed by rapid drying due to the arid nature of the region, but it would not necessarily enter drought (in Fig. 10, the peak in rapid intensification occurs in July when the Intermountain West is included which is shortly after or during monsoon season whereas the peak occurs in August and September east of the Rocky Mountains). It is also feasible that drought depiction by SESR may be limited in the Intermountain

West due to the inherent arid nature of the region, emphasis on ET, and the role of winter precipitation instead of summer precipitation (Otkin et al., 2014) at higher elevations, which could lead to the frequent misses in drought identification. Finally, it is also possible this might be a reanalysis and resolution issue due to the complex topography of the region. Overall, there are several potential reasons why a high frequency of rapid intensification events west of the Rocky Mountains exist with limited drought occurrence, and future work is needed to determine the physical mechanisms.

With regards to the drought component, SESR has the potential to identify drought as an individual metric. It successfully represented the spatial extent of drought events and identified areas where the drought is most extreme. For example, SESR was able to accurately depict the spatial extent of the 2011 drought found in Vicente-Serrano et al. (2018) and Kim et al. (2019). However, SESR was found to underestimate drought severity and its persistence. That is, SESR may be sensitive to moderating events (precipitation, cooler temperatures, etc.) and no longer identifies drought after such events even when impacts are still present. This effect with a noisy precipitation and temperature record has also been noted in Osman et al. (2021). It should be noted here that there is some level of subjectivity in the USDM (Leasor et al., 2020) and that the USDM uses multiple indices for a convergence of evidence across multiple time scales to identify drought (McEvoy et al., 2016), whereas SESR identifies rapidly changing drought across a pentad timescale. That is, the USDM represents agricultural and hydrologic drought, whereas SESR represents more meteorological and agricultural drought. Thus, areas that experienced more long-duration droughts (e. g., Georgia and the Intermountain West in the past 20 years) will not see as much agreement between SESR and the USDM. But SESR is able to depict rapidly deteriorating conditions.

On a climatological scale, SESR continued to demonstrate strong potential in being able to identify drought, consistently identifying drought in the Pacific Northwest, the Northern and Central Plains, the majority of the Deep South, the Great Lakes Regions, and the Northeast. However, there was not much agreement between SESR and the USDM across arid and semi-arid regions and in regions of complex topography such as the Intermountain West and portions of the Southern Plains. There was also little agreement in Georgia and the Ohio River Valley. In addition to representing different types of drought, a possible explanation is that aridity and, to a lesser degree, temperature governs how well SESR and the USDM agreed. That is, SESR's lowest error (Fig. 12) was in more humid regions, whereas it struggled in more arid regions. Although aridity cannot explain the performance of SESR in all locations, (e.g., the low false positive and negative errors in the more arid Northern Plains and in Georgia) aridity serves as a proxy for the accuracy of drought representation by SESR compared to the USDM. Another notable result is that SESR performs well in regions that experience moderate to high transpiration (e.g., the Northern Plains and Pacific Northwest). If the vegetation conserves moisture, as conifers and most arid vegetation do, then ET may not be a good measure for vegetation health. This would explain the low false positive and negative errors in the Pacific Northwest, despite the importance of wintertime precipitation (which was excluded for this study), as it has more temperate vegetation that transpires more readily. It would also explain the low false positive and negative errors in the cultivated Northern Plains.

Lastly, the poor agreement between the USDM and SESR in the Intermountain West could also be related to hydrologic processes in that region. That is, the main precipitation in the Intermountain West is in snowpack during the winter, which SESR does not look at. Since SESR does not consider features such as river levels and snowpack, an additional metric would be useful to represent the hydrologic processes that occur in that region of the country. It is suggested that more work be done to investigate the reasons for why SESR succeeds and fails where it does.

The difficulty SESR showed in representing more long-term droughts, particularly in arid regions and in extreme scenarios, and

the fact that the percentiles can only identify D4 drought in one year out of the dataset given its relatively short period of record, suggests that it should have help from another index, variable, or dataset to help accurately represent drought. Because ET incorporates soil moisture, vegetation conditions, and general moisture conditions (Chen et al., 1996), and PET incorporates temperature and soil fluxes (Mahrt and Ek, 1984), the variable most indirectly represented by SESR is precipitation. Thus, a precipitation index such as SPI would be recommended to help identify drought.

5. Conclusion

This study utilized the method of flash drought identification developed by Christian et al. (2019b) and separated flash drought into (1) rapid intensification and (2) drought components. These components were examined separately to investigate their contribution to flash drought development for several different cases. Analysis of the drought component was completed by comparing the SESR results to the USDM from 2010 to 2019, and the rapid intensification component was compared to the results of previous studies.

This study provided key insights into mechanisms that contribute towards flash drought development. It was determined that rapid intensification component plays a prominent role in flash drought development east of the Rocky Mountains, whereas the drought component plays a more prominent role west of the Rocky Mountains. Therefore, attempts to identify flash drought in real time, or predict them must be able to capture rapidly developing drought conditions. In addition, SESR showed strong potential in being able to identify rapidly changing and short-term drought. It is recommended to investigate how the results of this method changes with different climatological periods (e.g., of use 10, 20, or 30 year averages instead of the 41-year average used in this study) to quantify how the results may vary under a changing climate. It is also recommended to investigate SESR's ability to identify drought in union with a precipitation index, such as SPI, to determine how effectively precipitation can accommodate for SESR's deficiencies in more long-term drought representation. Overall, this analysis was able to separate flash drought into components and provide a means to quantify rapid intensification and drought using SESR, providing a new way to examine flash drought events.

Declaration of Competing Interest

The authors declare that they have no known competing financial interests or personal relationships that could have appeared to influence the work reported in this paper.

Data availability

I have shared the link to my code at the Attach File Step. Large data files, e.g. for SESR or FD, are available on request.

Acknowledgements

Supplementary materials

Supplementary material associated with this article can be found, in the online version, at doi:10.1016/j.agrformet.2022.109288.

References

Anderson, M.C., Hain, C., Otkin, J., Zhan, X., Mo, K., Svoboda, M., Wardlow, B., Pimstein, A., 2013. An intercomparison of drought indicators based on thermal remote sensing and NLDAS-2 simulations with U.S. Drought Monitor classifications. J. Hydrometeorol. 14, 1035–1056. https://doi.org/10.1175/JHM-D-12-0140.1. https://doi.org/10.1175/JHM-D-12-0140.1.

Anderson, M.C., Norman, J.M., Mecikalski, J.R., Otkin, J.A., Kustas, W.P., 2007. A climatological study of evapotranspiration and moisture stress across the continental United States based on thermal remote sensing: 1. model formulation. J. Geophys. Res. 112 https://doi.org/10.1029/2006JD007506. https://doi.org/10.1029/2006JD007506.

American Meteorological Society, A. M. S., 1997. Meteorological drought-policy statement. Bull. Am. Meteorol. Soc. 78, 847–849.

Basara, J.B., Christian, J.I., Wakefield, R.A., Otkin, J.A., Hunt, E.H., Brown, D.P., 2019. The evolution, propagation, and spread of flash drought in the central United States during 2012. Environ. Res. Lett. 14 (8), 084025 https://doi.org/10.1088/1748-9326/ab2cc0. https://doi.org/10.1088/1748-9326/ab2cc0.

Bolles, K.C., Williams, A.P., Cook, E.R., Cook, B.I., Bishop, D.A., 2021. Tree-ring reconstruction of the atmospheric ridging feature that causes flash drought in the central United States since 1500. Geophys. Res. Lett. 48 (4) https://doi.org/10.1029/2020gl091271. https://doi.org/10.1029/2020GL091271.

Chen, F., Coauthors, 1996. Modeling of land surface evaporation by four schemes and comparison with fife observations. J. Geophys. Res. 101 (D3), 7251–7268.

Chen, L.G., Gottschalck, J., Hartman, A., Miskus, D., Tinker, R., Artusa, A., 2019. Flash drought characteristics based on U.S. drought monitor. Atmosphere 10 (9), 498. https://doi.org/10.3390/atmos10090498. https://doi.org/10.3390/atmos10090498.

Christian, J.I., Basara, J.B., Lowman, L.E.L., Xiao, X., Mesheske, D., Zhou, Y., 2022. Flash drought identification from satellite-based land surface water index. Remote Sens. Appl. 26, 100770.

Christian, J.I., Basara, J.B., Hunt, E.D., Otkin, J.A., Furtado, J.C., Mishra, V., Xiao, X., Randall, R.M., 2021. Global distribution, trends, an drivers of flash drought occurrence. Nat. Commun. 12, 6330. https://doi.org/10.1038/s41467-021-26692-z. https://doi.org/10.1038/s41467-021-26692-z.

Christian, J.I., Basara, J.B., Hunt, E.D., Otkin, J.A., Xiao, X., 2020. Flash drought development and cascading impacts associated with the 2010 Russian heatwave. Environ. Res. Lett. 15 (9), 094078 https://doi.org/10.1088/1748-9326/ab9faf. https://doi.org/10.1088/1748-9326/ab9faf.

Christian, J.I., Basara, J.B., Otkin, J.A., Hunt, E.D., 2019a. Regional characteristics of flash droughts across the United States. Environ. Res. Commun. 1 (12), 125004 https://doi.org/10.1088/2515-7620/ab50ca. https://doi.org/10.1088/2515-7620/ab50ca.

Christian, J.I., Basara, J.B., Otkin, J.A., Hunt, E.D., Wakefield, R.A., Flanagan, P.X., Xiao, X., 2019b. A methodology for flash drought identification: Application of flash drought frequency across the United States. J. Hydrometeorol. 20 (5), 833–846. https://doi.org/10.1175/jhm-d-18-0198.1. https://doi.org/10.1175/JHM-D-18-0198.1.

Dai, A., 2011. Characteristics and trends in various forms of the palmer drought severity index during 1900–2008. J. Geophys. Res. 116 (D12) https://doi.org/10.1029/2010jd015541. https://doi.org/10.1029/2010JD015541.

Ek, M.B., Mitchell, K.E., Lin, Y., Rogers, E., Grunmann, P., Koren, V., Gayno, G., Tarpley, J.D., 2003. Implementation of Noah land surface model advances in the National Centers for Environmental Prediction operational mesoscale eta model. J. Geophys. Res. 108 (D22) https://doi.org/10.1029/2002jd003296. https://doi.org/10.1029/2002JD003296.

Flanagan, P.X., Basara, J.B., Illston, B.G., Otkin, J.A., 2017. The effect of the dry line and convective initiation on drought evolution over Oklahoma during the 2011 drought. Adv. Meteorol. 2017, 1–16. https://doi.org/10.1155/2017/8430743. https://doi.org/10.1155/2017/8430743.

Ford, T.W., McRoberts, D.B., Quiring, S.M., Hall, R.E., 2015. On the utility of in situ soil moisture observations for flash drought early warning in Oklahoma, USA. Geophys. Res. Lett. 42 (22), 9790–9798. https://doi.org/10.1002/2015gl066600. https://doi.org/10.1002/2015GL066600.

Heim, R.R., 2002. A review of twentieth-century drought indices used in the United States. Bull. Am. Meteorol. Soc. 83 (8), 1149–1166. https://doi.org/10.1175/1520-0477-83.8.1149. https://doi.org/10.1175/1520-0477-83.8.1149.

Hobbins, M.T., Wood, A., McEvoy, D.J., Huntington, J.L., Morton, C., Anderson, M., Hain, C., 2016. The evaporative demand drought index. Part I: Linking drought evolution to variations in evaporative demand. J. Hydrometeorol. 17 (6), 1745–1761. https://doi.org/10.1175/jhm-d-15-0121.1. https://doi.org/10.1175/JHM-D-15-0121.1.

Hunt, E.D., Femia, F., Werrell, C., Christian, J.I., Otkin, J.A., Basara, J., Anderson, M., White, T., Hain, C., Randall, R., McGaughey, R., 2021. Agricultural and food security impacts from the 2010 Russia flash drought. Weather Climate Extremes 34, 100383. https://doi.org/10.1016/j.wace.2021.100383, 10.1016/j.wace.2021.100383.

Hunt, E.D., Birge, H.E., Laingen, C., Licht, M.A., McMechan, J., Baule, W., Connor, T., 2020. A perspective on changes across the U.S. corn belt. Environ. Res. Lett. 15 (7) https://doi.org/10.1088/1748-9326/ab9333, 10.1088/1748-9326/ab9333.

Hunt, E.D., Hubbard, K.G., Wilhite, D.A., Arkebauer, T.J., Dutcher, A.L., 2009. The development and evaluation of a soil moisture index. Int. J. Climatol. 29 (5), 747–759. https://doi.org/10.1002/joc.1749. https://doi.org/10.1002/joc.1749.

Hunt, E.D., Svoboda, M., Wardlow, B., Hubbard, K., Hayes, M., Arkebauer, T., 2014. Monitoring the effects of rapid onset of drought on non-irrigated maize with agronomic data and climate-based drought indices. Agric. For. Meteorol. 191, 1–11. https://doi.org/10.1016/j.agrformet.2014.02.001. https://doi.org/10.1016/j.agrformet.2014.02.001.

Kim, D., Lee, W., Kim, S.T., Chun, J.A., 2019. Historical drought assessment over the contiguous united states using the generalized complementary principle of evapotranspiration. Water Resour. Res 55 (7), 6244–6267. https://doi.org/10.1029/2019wr024991. https://doi.org/10.1029/2019WR024991.

Kim, D., Rhee, J., 2016. A drought index based on actual evapotranspiration from the bouchet hypothesis. Geophys. Res. Lett. 43 (19) https://doi.org/10.1002/2016gl070302, 10,277–10,285URL. https://doi.org/10.1002/2016GL070302.

Leasor, Z.T., Quiring, S.M., Svoboda, M.D., 2020. Utilizing objective drought severity thresholds to improve drought monitoring. J. Appl. Meteorol. Climatol. 59 (3), 455–475. https://doi.org/10.1175/jamc-d-19-0217.1. https://doi.org/10.1175/JAMC-D-19-0217.1.

Li, J., Wang, Z., Wu, X., Xu, C.-Y., Guo, S., Chen, X., 2020. Toward monitoring short-term droughts using a novel daily scale, standardized antecedent precipitation evapotranspiration index. J. Hydrometeorol. 21 (5), 891–908. https://doi.org/10.1175/jhm-d-19-0298.1. https://doi.org/10.1175/JHM-D-19-0298.1.

Lisonbee, J., Woloszyn, M., Skumanich, M., 2021. Making sense of flash drought: definitions, indicators, and where we go from here. J. Appl. Service Climatol. 2021 (1), 1–19. https://doi.org/10.46275/joasc.2021.02.001. https://doi.org/10.46275/JOASC.2021.02.001.

Liu, Y., Zhu, Y., Ren, L., Otkin, J., Hunt, E.D., Yang, X., Yuan, F., Jiang, S., 2020a. Two different methods for flash drought identification: Comparison of their strengths and limitations. J. Hydrometeorol. 21 (4), 691–704. https://doi.org/10.1175/jhm-d-19-0088.1. https://doi.org/10.1175/JHM-D-19-0088.1.

Liu, Y., Zhu, Y., Zhang, L., Ren, L., Yuan, F., Yang, X., Jiang, S., 2020b. Flash droughts characterization over China: From a perspective of the rapid intensification rate. Sci. Total Environ. 704, 135373 https://doi.org/10.1016/j.scitotenv.2019.135373, 10.1016%2Fj.scitotenv.2019.135373.

Mahrt, L., Ek, M., 1984. The influence of atmospheric stability on potential evaporation. J. Clim. Appl. Meteorol. 23 (2), 222...234 URL doi:10.1175/1520-0450(1984)023<0222:tioaso>2.0.co;2. https://doi.org/10.1175/1520-0450(1984)023<0222:TIOASO>2.0.CO;2.

McEvoy, D.J., Huntington, J.L., Hobbins, M.T., Wood, A., Morton, C., Anderson, M., Hain, C., 2016. The evaporative demand drought index. Part II: CONUS-wide assessment against common drought indicators. J. Hydrometeorol. 17 (6), 1763–1779. https://doi.org/10.1175/jhm-d-15-0122.1. https://doi.org/10.1175/jhm-d-15-0122.1.

McKee, T.B., Doesken, N.J., Kleist, J., 1995. Drought monitoring with multiple time scales. In: Proceedings of the 9th Conference on Applied Climatology.

McKee, T.B., Doesken, N.J., Kleist, J., Coauthors, 1993. The relationship of drought frequency and duration to time scales. In: Proceedings of the 8th Conference on Applied Climatology. Boston, pp. 179–183. Vol. 17.

Mesinger, F., Coauthors, 2006. North American Regional Reanalysis. Bull. Am. Meteorol. Soc. 87 (3), 343–360. https://doi.org/10.1175/bams-87-3-343. https://doi.org/10.1175/BAMS-87-3-343.

National Centers for Environmental Information, 2017: Billion-dollar weather and climate disasters: Overview. URL https://www.ncdc.noaa.gov/billions/.

Nguyen, H., Wheeler, M.C., Hendon, H.H., Lim, E.P., Otkin, J.A., 2021. The 2019 flash droughts in subtropical eastern Australia and their association with large-scale climate drivers. Weather Climate Extremes 32, 100321. https://doi.org/10.1016/j.wace.2021.100321. https://doi.org/10.1016/j.wace.2021.100321.

Nguyen, H., Wheeler, M.C., Otkin, J.A., Cowan, T., Frost, A., Stone, R., 2019. Using the evaporative stress index to monitor flash drought in Australia. Environ. Res. Lett. 14, 064016 https://doi.org/10.1088/1748-9326/ab2103. https://doi.org/10.1088/1748-9326/ab2103.

Noguera, I., Domínguez-Castro, F., Vicente-Serrano, S.M., 2020. Characteristics and trends of flash droughts in Spain, 1961–2018. Ann. N.Y. Acad. Sci. 1472 (1), 155–172. https://doi.org/10.1111/nyas.14365. https://doi.org/10.1111/nyas.14365.

Osman, M., Zaitchik, B.F., Badr, H.S., Christian, J.I., Tadesse, T., Otkin, J.A., Anderson, M.C., 2021. Flash drought onset over the contiguous United States: sensitivity of inventories and trends to quantitative definitions. Hydrol. Earth Syst. Sci. 25, 565–581. https://doi.org/10.5194/hess-25-565-2021, 10.5194/hess-25-565-2021.

Otkin, J.A., Anderson, M.C., Hain, C., Mladenova, I.E., Basara, J.B., Svoboda, M., 2013. Examining rapid onset drought development using the thermal infrared–based evaporative stress index. J. Hydrometeorol. 14 (4), 1057–1074. https://doi.org/10.1175/jhm-d-12-0144.1. https://doi.org/10.1175/JHM-D-12-0144.1.

Otkin, J.A., Anderson, M.C., Hain, C., Svoboda, M., 2014. Examining the relationship between drought development and rapid changes in the evaporative stress index. J. Hydrometeorol. 15 (3), 938–956. https://doi.org/10.1175/jhm-d-13-0110.1. https://doi.org/10.1175/JHM-D-13-0110.1.

Otkin, J.A., Anderson, M.C., Hain, C., Svoboda, M., Johnson, D., Mueller, R., Tadesse, T., Wardlow, B., Brown, J., 2016. Assessing the evolution of soil moisture and vegetation conditions during the 2012 United States flash drought. Agric. For. Meteorol. 218-219, 230–242. https://doi.org/10.1016/j.agrformet.2015.12.065. https://doi.org/10.1016/j.agrformet.2015.12.065.

Otkin, J.A., Svoboda, M., Hunt, E.D., Ford, T.W., Anderson, M.C., Hain, C., Basara, J.B., 2018. Flash droughts: a review and assessment of the challenges imposed by rapid-onset droughts in the united states. Bull. Am. Meteorol. Soc. 99 (5), 911–919. https://doi.org/10.1175/bams-d-17-0149.1. https://doi.org/10.1175/BAMS-D-17-0149.1.

Otkin, J.A., Zhong, Y., Hunt, E.D., Basara, J., Svoboda, M., Anderson, M.C., Hain, C., 2019. Assessing the evolution of soil moisture and vegetation conditions during a flash drought–flash recovery sequence over the south-central united states. J. Hydrometeorol. 20 (3), 549–562. https://doi.org/10.1175/jhm-d-18-0171.1. https://doi.org/10.1175/JHM-D-18-0171.1.

Otkin, J.A., Zhong, Y., Hunt, E.D., Christian, J.I., Basara, J.B., Nguyen, H., Wheeler, M.C., Ford, T.W., Hoell, A., Svoboda, M., et al., 2021. Development of a flash drought intensity index. Atmosphere 12, 741. https://doi.org/10.3390/atmos12060741. https://doi.org/10.3390/atmos12060741.

Pachauri, R.K., Coauthors, 2014. Climate Change 2014: Synthesis Report. Contribution of Working Groups I, II and III to the Fifth Assessment Report of the Intergovernmental Panel on Climate Change. IPCC, Geneva, Switzerland.

Palmer, W.C., 1965. Meteorological Drought. U.S. Department of Commerce, Weather Bureau. Vol. 30.

Pendergrass, A.G., Coauthors, 2020. Flash droughts present a new challenge for subseasonal-to-seasonal prediction. Nature Climate Change 10 (3), 191–199. https://doi.org/10.1038/s41558-020-0709-0. https://doi.org/10.1038/s41558-020-0709-0.

Svoboda, M., Coauthors, 2002. The drought monitor. Bull. Am. Meteorol. Soc. 83 (8), 1181–1190. https://doi.org/10.1175/1520-0477-83.8.1181. https://doi.org/10.1175/1520-0477-83.8.1181.

Vicente-Serrano, S.M., Coauthors, 2018. Global assessment of the standardized evapotranspiration deficit index (SEDI) for drought analysis and monitoring. J. Climate 31 (14), 5371–5393. https://doi.org/10.1175/jcli-d-17-0775.1. https://doi.org/10.1175/JCLI-D-17-0775.1.